Platelet retraction force measurements using flexible post force sensors

Xin M. Liang,[a] Sangyoon J. Han,[a] Jo-Anna Reems,[b] Dayong Gao*[a] and Nathan J. Sniadecki*[a]

Received 11th September 2009, Accepted 21st December 2009
First published as an Advance Article on the web 20th January 2010
DOI: 10.1039/b918719g

Platelets play an important role in hemostasis by forming a thrombotic plug that seals the vessel wall and promotes vascular healing. After platelets adhere and aggregate at the wound site, their next step is to generate contractile forces through the coordination of physicochemical interactions between actin, myosin, and $\alpha_{IIb}\beta_3$ integrin receptors that retract the thrombus' size and strengthen its adhesion to the exposed matrix. Although platelet contractile forces (PCF) are a definitive feature of hemostasis and thrombosis, there are few approaches that can directly measure them. In this study, we describe the development of an approach to measure PCF in microthrombi using a microscopic flexible post force sensor array. Quasi-static measurements and live microscopic imaging of thrombin-activated platelets on the posts were conducted to assay the development of PCF to various hemostatic conditions. Microthrombi were observed to produce forces that monotonically increased with thrombin concentration and activation time, but forces subsided when thrombin was removed. PCF results were statistically similar on arrays of posts printed with fibronectin or fibrinogen. PCF measurements were combined with clot volume measurements to determine that the average force per platelet was 2.1 ± 0.1 nN after 60 min, which is significantly higher than what has been measured with previous approaches. Overall, the flexible post arrays for PCF measurements are a promising approach for evaluating platelet functionality, platelet physiology and pathology, the impacts of different matrices or agonists on hemostatic responses, and in providing critical information regarding platelet activity that can guide new hemostatic or thrombotic strategies.

Introduction

Platelets are highly specialized discoid-shaped cells that play an essential role in hemostatic response.[1] Platelets can roll along the surface of endothelial cells,[2] but when the integrity of the endothelial layer is damaged, intimal matrix proteins are exposed that trigger rapid platelet adhesion and initiate thrombus formation.[3] Initially, platelets are loosely bound together in the thrombus through $\alpha_{IIb}\beta_3$ integrin receptors that bind to multivalent molecular ligand bridges.[4–6] Following the aggregation phase, thrombus retraction reduces the size of the structure and stabilizes its structural integrity.[4] Although the mechanisms of thrombus stability are not fully understood, it may arise through compaction of the space between platelets to increase local agonist concentration,[5] strain-hardening of the surrounding fibrin mesh to prevent fibrinolysis,[7] or possibly through transduction of platelet contractile forces that elicit increases in integrin adhesion strength.[8]

The interaction between actin and non-muscle myosin IIA that generates contractile forces in platelets is essential to thrombus retraction and stability.[9] Actin undergoes rapid polymerization during activation that promotes shape change and leads to formation of filaments that connect to integrin $\alpha_{IIb}\beta_3$ through focal adhesion proteins.[10–12] Without sufficient myosin force generation, platelets are impaired in their hemostatic role.[13–15] Platelet contractile forces (PCF) are significantly suppressed when general inhibitors of thrombosis like heparin, aspirin, and $\alpha_{IIb}\beta_3$ blockers are used.[16] These findings raise the possibility that direct measurement of PCF can be used to evaluate hemostatic risk.

The majority of functional assays for platelets focus on early stage parameters in the hemostatic response[17,18] or on the viscoelastic properties of the thrombus[19,20] and do not focus on myosin motor activity. So far, two types of approaches have been reported that directly measure PCF.[21–24] The first approach forms a macroscale clot strip which has one end anchored and the other end tied to a force transducer to measure the isometric load generated when platelets are activated.[21,23] The second approach measures the downward force as a clot is formed from whole blood or platelet-rich plasma between two parallel plates, one of which is connected to a force transducer.[22,24] These techniques have shown a correlation between platelet functionality and PCF that is important in evaluating risk factors and medical treatments.[16,25,26] There is a structural relationship between the platelet cytoskeleton and the surrounding fibrin meshwork,[23,27,28] but due to the macroscopic size of current PCF approaches, the coupled effects of passive fibrin elasticity and active platelet forces convolute the force measurement. Moreover, these closed systems do not allow for visual monitoring of thrombus formation, which can reveal key biophysical events that occur in the process. Overcoming the current limitations in force transducer resolution and sensitivity can circumvent the restrictions and lead to insights into hemostasis and thrombosis that arise from studying PCF.

In this study, we present an approach to directly measure PCF that has been adapted from a previous technique for measuring

[a]*Department of Mechanical Engineering, University of Washington, Seattle, USA. E-mail: nsniadec@uw.edu; dayong@uw.edu*
[b]*Puget Sound Blood Center, Seattle, USA*

traction forces of cells using arrays of flexible, vertical posts.[29,30] The posts are made from a silicone elastomer and deflect like cantilever springs that directly report the local force by the degree of tip deflection. Fibrinogen or fibronectin were microcontact printed onto the tips of the posts to enable platelet adhesion and to examine the thrombotic potential of these ligands for aggregation and PCF generation. Thrombin concentration was assayed to achieve a condition of maximum platelet contractility. Results were compared between quasi-static approaches and live imaging of thrombus formation to demonstrate the potential of the technique in monitoring platelet functionality and thrombosis in a spatio-temporal manner.

Methods and materials

Reagents

Human fibrinogen (plasminogen depleted) and human α-thrombin were obtained from Enzyme Research Laboratories. Human fibronectin was obtained from BD Biosciences. Alexa Fluor 488 phalloidin and fluorescent 1,1′-dioleyl-3,3,3′,3′-tetramethylindocarbo-cyanine methanesulfonate (DiI) were obtained from Invitrogen. CGS washing buffer contained 120 mM NaCl, 13 mM sodium citrate, and 30 mM glucose at pH 7. Tyrode buffer contained 10 mM HEPES, 138 mM NaCl, 5.5 mM glucose, 12 mM $NaHCO_3$, 0.36 mM Na_2HPO_4, 2.9 mM KCl, 0.4 mM $MgCl_2$ and 0.8 mM $CaCl_2$ at pH 7.5.

Subjects

Under a protocol approved by the Human Subject Division at University of Washington, written informed consent was obtained from all volunteer subjects. Volunteers with no previously known platelet abnormality and had not received any anti-platelet medication in the two weeks prior to sample collection participated in this study.

Sample preparation

Human whole blood was collected from healthy volunteers by licensed professionals at the University of Washington Medical Center Blood Draw Lab. The blood samples were anti-coagulated in blood collection tubes containing acid-citrate-dextrose (ACD) solution A (1.5 ml of ACD to 8.5 ml whole blood). Platelet-rich plasma (PRP) was obtained from anti-coagulated whole blood by centrifugation at 120 × *g* for 20 min. After the soft-spin, 1 ml of CGS buffer was added to 9 ml of PRP. The diluted PRP was centrifuged at 1200 × *g* for 10 min. After the hard-spin, the working suspension was obtained by re-suspending platelet pellet in Tyrode buffer and platelet count was performed using a Coulter counter in order to obtain a concentration of 5×10^7 platelets per ml.

Sensor fabrication and biofunctionalization

We have adopted our previously reported technique for fabricating arrays of vertical posts made from polydimethylsiloxane (PDMS, Sylgard 184, Dow Corning).[31] Briefly, PDMS posts were fabricated through a replica-molding process from an SU-8 silicon master. Fibrinogen or fibronectin (50 μg ml^{-1}) was adsorbed onto flat PDMS stamps for 1 h, dried under N_2, and then placed into contact with ozone-treated post arrays. Intimate contact between the posts and the stamp allows protein to transfer onto the tips of the posts. Substrates were then submerged in DiI solution (10 μg ml^{-1}) for 2 h to absorb the hydrophobic dye into the posts for fluorescence microscopy imaging. The arrays were treated for 2 h in 0.2% Pluronics F-127 NF solution (BASF) to block the sidewalls of the posts, as well as the bottom surface of the array. When platelets were later added onto the post arrays, the previous biofunctional treatments with printed adhesive matrix proteins and non-adhesive Pluronics coating confined platelet adhesion to only the tips, yielding more accurate force measurements.

Quasi-static platelet contractile force measurements

The posts of each array (Fig. 1A) were fully submerged into 10 ml of Tyrode buffer in a 60 mm dish, followed by the addition of varied volume of platelet suspension to reach a density between 1 and 2×10^7 platelets per ml, and allowed to equilibrate for 25 min before stimulation (Fig. 1B). Platelets were activated

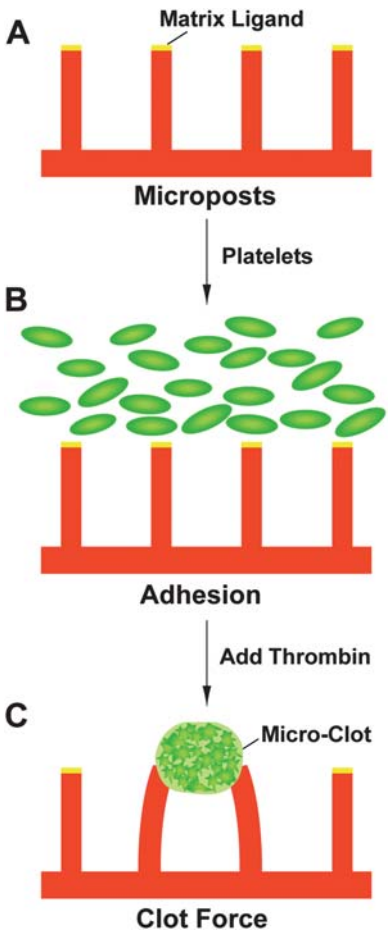

Fig. 1 Experimental flow schematic of platelet contractile force measurements. (A) Micropost arrays are printed with matrix ligand and fully submerged in Tyrode buffer. (B) Platelets in Tyrode buffer are added onto the arrays and allowed to settle to the bottom. (C) Thrombin is added to activate the platelets, which induces microthrombus formation and contraction.

using thrombin at different concentrations to induce thrombus formation (0, 0.1, 1, 3.5, or 10 U ml^{-1}) (Fig. 1C). After thrombin was added, the samples were left undisturbed for a predefined time before fixing with 4% paraformaldehyde and subsequent immunofluorescence staining steps. A similar set of experiments were conducted where platelets were stimulated with 3.5 U ml^{-1} of thrombin for 0, 5, 10, 30, and 60 min on arrays coated with fibronectin. A set of washout experiments were also conducted where the platelets were activated for 30 min or 60 min and then transferred to a new dish containing Tyrode buffer but without free platelets or thrombin in solution. The platelets on the arrays were left undisturbed for an additional 30 or 60 min before fixing and staining.

Platelet actin was counterstained with Alexa Fluor 488 phalloidin. The posts were fluorescently labeled with DiI during the biofunctional preparation. A Zeiss LSM 510 confocal microscope with a high-magnification objective (63× oil) was used to obtain Z-section images of the microthrombi on the posts at 0.4 μm increments (Fig. 2A). This method provided an accurate measurement of post deflections because the location of the top and bottom images can be precisely determined. A previously reported image analysis routine written in MATLAB (Mathworks) was used to calculate the centroid position of the top and bottom of the posts.[32] The direction and magnitude of each post deflection ($\vec{x}$) can be found from the difference in positions of the top *versus* bottom of each post. The contractile force at each post is calculated by the cantilever equation:

$$\vec{F} = \left(3\pi ED^4/64L^3\right)\vec{x} \quad (1)$$

where E is the modulus of elasticity of PDMS, post diameter was $D = 2.2$ μm, and post height was either $L = 6.2$ μm or 7.0 μm. A sample outcome of the image analysis is shown in Fig. 2B. The total contraction force of each thrombus clot was calculated by summation of the magnitude of $\vec{F}$ for each post attached to it. To ensure accuracy of the measurements, microthrombi with a vector-sum imbalance in force greater than 4 nN were excluded.

The modulus of elasticity of PDMS was measured according to ASTM standard D412 using a dumbbell-shaped specimen that was baked for 14 h at 100 °C and tested on an Instron machine with a 1 kN load cell and 0.2 mm s^{-1} extension rate. The thicknesses of the dumbbell-shaped specimens were measured before testing and found to be 1.60 ± 0.03 mm. For extension data, felt-pen marks on two distant ends of the gage portion were measured using caliper for initial and extended final lengths for 5% strain. A linear stress–strain relationship was used with the force-extension data to determine that modulus of elasticity of PDMS is $E = 2.86 \pm 0.03$ MPa.

Image analysis was performed in MATLAB by using the Z-sectioned images of phalloidin-labeled actin to determine the clot volume. For each image in a Z-stack, the pixel area inside the microthrombus' circumference was tallied. The total pixel area for all images in a Z-stack was then converted to cubic micrometres by converting pixel area to square micrometres and then by multiplying by the Z-step increment of 0.4 μm. For the number of platelets in a thrombus, a similar approach was used, but a thresholding filter was applied to the actin image to identify the platelets inside a microthrombus. The total pixel count was then converted to cubic micrometres as before. The number of platelets in a clot was then determined by assuming that an average platelet maintains a constant volume of ~9 fl.[17,18]

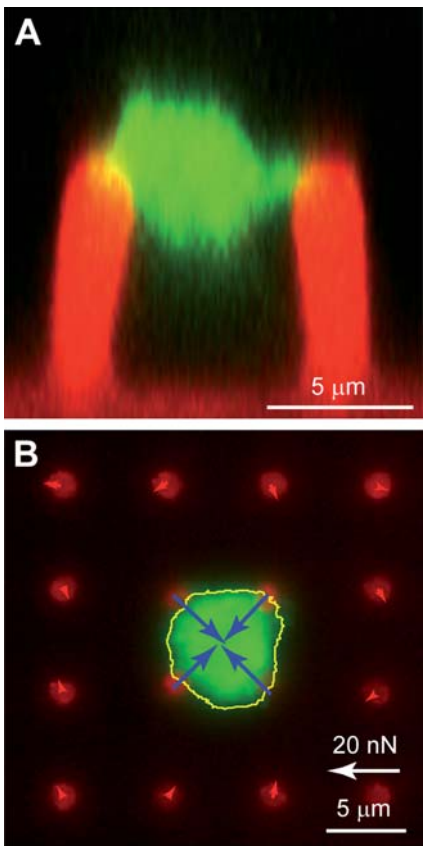

Fig. 2 Measurement of platelet forces and thrombus volume. (A) Side view image of microthrombus attached to two posts was generated from a Z-stack series of confocal microscopy images. The PDMS of the posts has been stained with DiI (red) and platelet actin with phalloidin (green). The bulk of the thrombus structure lie in between the posts and is connected at the tips of the posts. The volume of the clot is measured by voxel measurements of the actin signal in the Z-stack. (B) Example of contraction force measurements using quasi-static technique. The outline of the clot (yellow line) and its contractile forces (blue arrows) have been determined by image analysis of the post deflections. There is good signal-to-noise in the approach as indicated by the low forces (red arrows) at the posts surrounding the clot.

Statistical analysis of data

To ensure reliability and repeatability in the approach, two experiments per thrombin concentration condition were performed for fibrinogen-coated arrays and three experiments for fibronectin-coated arrays. Two-way ANOVA tests revealed significant statistical dependence to thrombin concentration ($p < 0.0001$ for both fibrinogen-coated and fibronectin-coated experiments) and no statistical difference between experiments ($p > 0.55$ for fibrinogen-coated experiments and $p > 0.67$ for fibronectin-coated experiments). For experiments on measuring the development of PCF within a 1 h period using constant thrombin concentration (3.5 U ml^{-1}), three sets of experiments per condition were performed on fibronectin-coated arrays. Similarly, two-way ANOVA tests showed significant dependence to time after activation ($p < 0.0001$) and no statistical difference

between the three experiments ($p > 0.35$). A single repetition was conducted for the washout experiments and no statistical difference was found when the contractile forces at 30 or 60 min of activation were compared to those of the previous three experiments ($p > 0.05$, Student's t-test). Taken together, the statistical analyses of the data revealed trends in PCF with respect to concentration and time that are without the adverse effect of donor-to-donor variability in platelet function.

Live thrombus contractility procedure

For live microscopy measurements, a substrate preparation similar to the quasi-static approach was used, but the formation of microthrombi and their deflections of the posts were video-recorded for spatio-temporal analysis. Arrays coated with fibronectin on the tips of the posts were fully submerged in platelet-Tyrode solution (1 to 2×10^7 platelets per ml) in a 60 mm dish, and kept undisturbed for 25 min while on a Nikon Ti-E inverted fluorescent microscope. Both phase-contrast and DiI fluorescent images were taken every 5 min with a 20× objective and cooled CCD camera connected to a computer with Nikon Elements imaging software. Thrombin at 3.5 U ml^{-1} was added 30 s prior to the 25 min mark, so that an image immediately after activation could be obtained. All images were acquired at a focal plane that lies at the tip of the posts. Deflections of the posts in the DiI image were measured using a previously developed program in IGOR (Wavemetrics) for live imaging analysis.[33] Briefly, the posts surrounding a thrombus were used as reference points to interpolate the undeflected positions of the posts. For live image analysis, thrombus formation was observed *via* phase-contrast microscopy and occurred immediately upon adding thrombin (Fig. 6A). Once a visible microthrombus was located, its posts were selected for image analysis for all time points before and after activation. Force calculations of these posts were added together to calculate the total contractile force that the clot generated in each time frame. Total force calculations were conducted throughout the entire experiment duration, even before thrombin was added, to establish the base lines for the platelet contractility graph.

Results

Comparison of matrix ligand and maximum platelet contractile activation

To ensure platelets were under conditions of maximal activation for PCF measurements, we initially studied the relationship between platelet contractility and thrombin concentration using a quasi-static measurement approach. To replicate the adhesive interactions of exposed matrix or fibrin meshwork, the tips of the posts were coated with fibrinogen. Platelets were seeded onto the post arrays and allowed to settle for 25 min prior to activation with a predefined concentration of thrombin (0, 0.1, 1, 3.5 or 10 U ml^{-1}) (Fig. 1). After 30 min, the samples were then fixed and stained for confocal microscopy imaging. Z-sectional images of the microthrombi revealed that aggregated platelets span the open space between two or more posts and are attached at points of fibrinogen coating on the tips of the posts (Fig. 2A). Although the bulk of the clot lies above and below the plane of the tips of the posts, there was no visual adhesion of the clot to the Pluronics-coated sidewalls of the posts, which indicates that the cantilever equation is well-suited for calculating the forces generated by the platelets.

At least fourteen microthrombi were analyzed at each thrombin concentration assayed on the fibrinogen-coated arrays (Fig. 3A). The addition of thrombin caused the platelets to generate forces that were larger than when no thrombin (0 U ml^{-1}) was added to the system. The total force of the platelets increased with higher thrombin concentrations, which indicates a trend in platelet force generation and thrombin concentration ($p < 0.0001$, ANOVA). For 3.5 and 10 U ml^{-1} thrombin, total force increased by an increment that was statistically insignificant ($p > 0.05$, Tukey's post-hoc test). The similar PCF response between the two higher thrombin concentrations suggests that thrombin may have a saturating effect for concentrations at or greater than 3.5 U ml^{-1}.

Thrombin is a major agonist that directly activates platelets through G-protein coupled receptors, but also converts fibrinogen to fibrin, which causes rapid encapsulation of both activated and inactivated platelets into a fiber meshwork.[34] Therefore, a set of experiments using fibronectin as the tip-coating were conducted to sidestep the effect of fibrin polymerization at the tips of the posts. Since both fibronectin and fibrinogen are ligands for $\alpha_{IIb}\beta_3$ integrins, the adhesive engagement to the actin–myosin contractile apparatus in the platelet cytoskeleton is expected to be similar. With fibronectin-coated tips, measurements of platelet contractile forces *versus* thrombin concentration were repeated with at least twelve microthrombi analyzed per condition (Fig. 3A). A similar increasing trend with thrombin concentration was observed with fibronectin, which confirms that both ligands serve as adhesive matrices that support similar levels of contractile forces and that the contraction *versus* concentration response is matrix independent ($p > 0.28$, two-way ANOVA). Since platelets can release adhesive molecules from their α granules, it is possible that other ligand molecules in addition to fibrinogen or fibronectin may be involved in the formation of microthrombi and platelet forces.

Under conditions of no thrombin addition, microthrombi formed on the arrays and produced non-zero forces for both ligand coatings. Engagement of integrin $\alpha_{IIb}\beta_3$ to fibrinogen can induce platelet adhesion, shape change, and aggregation without the presence of exogenic agonists.[35] The non-zero forces observed with the micropost arrays indicate that both ligands can also induce thrombus formation and a retraction response. It is also possible that platelet activation and aggregation could have been

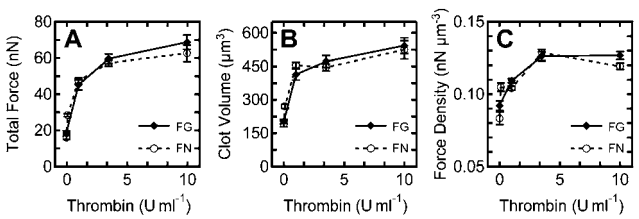

Fig. 3 Platelet contractile forces are activated by thrombin concentration. (A) Total force increases with thrombin concentration on both fibrinogen and fibronectin tip coatings. (B) Clot volume as measured by confocal volume measurements increases with thrombin concentration. (C) Contractile force density is the ratio of total force to clot volume.

initiated by non-specific interactions while in contact with the surface of the post arrays. To address this, control experiments were conducted with arrays coated with Pluronics on the posts and without any matrix protein coatings, but microthrombi failed to form on these substrates. Thus, a likely explanation is that platelet adhesion *via* $\alpha_{IIb}\beta_3$ in conjunction with secreted agonists during shape change activated the platelets and induced weak contractile forces without exogenous thrombin.

Each microthrombus is composed of a different number of aggregated platelets and increases in thrombin concentration caused more platelet aggregation in addition to contractile forces. To assess platelet aggregation *versus* thrombin concentration, the volume of each clot was analyzed using a Z-sectioning approach that converted its pixel areal count in each image of a Z-stack to volumetric dimensions (Fig. 3B). Thrombin concentration was found to stimulate platelet aggregation as indicated by increased clot volume, but for both ligands there was a statistically insignificant increase in clot size for thrombin concentrations greater than 3.5 U ml^{-1} ($p > 0.05$, Tukey's post-hoc test). The data suggest that platelets are activated and aggregate together with increased thrombin concentration, but there were no significant increases in clot size for concentrations higher than 3.5 U ml^{-1}.

Since each clot varied in volume to a small degree, it was appropriate to compare the PCF data by normalizing the total force data by clot volume to obtain a measurement of force density in the clots. Similar to the total force and clot volume, force density increased with thrombin concentration for both ligand coatings (Fig. 3C). However, there were statistically insignificant changes in force density between 3.5 and 10 U ml^{-1} of thrombin ($p > 0.05$, Tukey's post-hoc test). The maximal contraction observed at higher thrombin concentrations suggests that platelets were sufficiently activated to generate actin–myosin forces at 3.5 U ml^{-1} of thrombin.

Quasi-static measurement of temporal clotting force generation

To examine the generation of PCF over time, platelets were seeded onto fibronectin-coated post arrays and activated with 3.5 U ml^{-1} of thrombin. Each sample was allowed to aggregate and form microthrombi for a predefined time before fixation (5, 10, 30, and 60 min) (Fig. 4A). Analysis of total force per thrombus revealed that PCF increased steadily over the course of 60 min. As before, the volume of each thrombus was analyzed using confocal microscopy Z-sectioning (Fig. 4B). The data indicate that the average clot volume increases with time, which suggests that free platelets in Tyrode solution aggregate steadily onto the thrombus and this leads to an accumulation of bulk size. Force density was also observed to increase with time (Fig. 4C). Taken together, it is likely that the increase in total force with time is due to increased generation of force by individual platelets and the incorporation of free platelets onto the microthrombus. After activation, there is an abundant amount of remaining platelets in solution and as time persists there is a greater chance that additional platelets will land on the microthrombus and aggregate together. Since each platelet can act as a contractile unit in the thrombus structure, accumulation of more platelets leads to an additive increase in total contractile force.

To circumvent the accumulation of platelets onto an existing thrombus, we conducted washout experiments where arrays with platelets were activated for 30 or 60 min with thrombin and then gently transferred to a new dish containing buffer without additional free platelets or thrombin. Microthrombi that formed on the arrays were kept undisturbed for an additional 30 or 60 min and then fixed and stained. At least seven microthrombi were analyzed at each time point. The removal of thrombin caused the total force to decrease with time after washout (Fig. 5A). The results also indicate that clot volume decreased with time due to clot retraction by the platelets (Fig. 5B). The loss in total force was more than the loss in clot volume resulting in force density to decrease with time (Fig. 5C). From confocal microscopy images of the microthrombi, it was observed that the clots reduced in volume and porosity with time after washout (Fig. 5D and E). As seen in the representative images shown, there were regions that were void of platelets inside many of the microthrombi before washout. Using a thresholding filter, it was determined that the volume of platelets in the microthrombi remained constant with time (Fig. 5B). The average number of platelets after 30 min of activation did not have statistically significant difference with time after washout ($p > 0.76$, ANOVA) nor did the number of platelets after 60 min of activation ($p > 0.9$ Student's t-test).

By estimating the number of platelets in each microthrombi, it was possible to analyze the force that an individual platelet produced (Fig. 5C). Similar to total force and force density, the

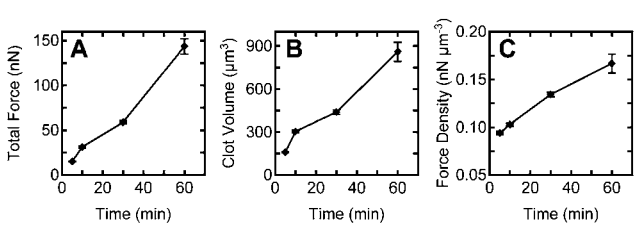

Fig. 4 Platelet contractile force generation increases steadily with time after thrombin addition. (A) Total force, (B) clot volume, and (C) force density increase in proportion to clotting time.

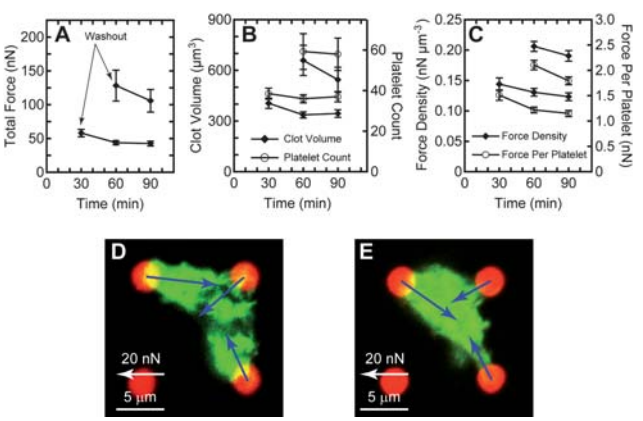

Fig. 5 Washout of freely floating platelets and thrombin causes platelet contractile forces to weaken. (A) Total force, (B) clot volume, and (C) force density decrease with time after washout. Confocal images of representative clots on the arrays are shown for (D) 30 min after activation and (E) 30 additional min after washout (60 min in total after activation).

force per platelet decreased with time after washout. However, the maximum force per platelet observed was 2.1 ± 0.1 nN, which is greater than what has been previously reported using macroscopic PCF approaches: ~7 pN per platelet after 20 min,[23] ~15 pN per platelet after 50 min,[27] ~0.3 nN per platelet after 17 min,[16,24] or ~0.5 nN per platelet after 80 min.[22] In comparison to traction forces of adherent cells, total force per platelet is significantly lower than the total force generated by nucleated cells (150–1000 nN per cell).[32] These macroscopic approaches have found that platelet contractility is temperature dependent and since all our experiments were conducted at room temperature, it is likely that platelet forces could be underreported in our approach. Since the quasi-static analysis approach does not track individual clot formation and force generation over time, more insights into thrombus formation with the quasi-static approach is limited. Thus, an approach for direct microscopic visualization and simultaneous live monitoring of PCF generation is necessary.

Live microthrombus contractility

To gain further insights into thrombus contraction, we extended the use of the flexible post arrays to live imaging on an inverted fluorescence microscope. This approach enables the monitoring of thrombus formation through phase-contrast microscopy (Fig. 6A). PCF development can also be monitored as before with the fluorescently labeled posts. Before thrombin is added, the platelets appear dark and similar in size to the posts. As before, thrombin was added after 25 min and microscopy imaging showed that microthrombi form rapidly on the posts. As time progresses, the clots produce larger contraction forces as indicated by the quiver arrows in the DiI image. A total of six microthrombi were recorded and the total force was measured for each captured time frame (Fig. 6B). The orange trace marks the force data for the thrombus shown in Fig. 6A.

From the video microscopy analysis, it was apparent that each microthrombus has different characteristics in clotting behavior and force generation dynamics. It was observed that platelets aggregated together and formed small clots while still suspended in solution before finally adhering onto the tip of the posts. Once in contact with ligands on the tips of the posts, these clots generate fast adhesion and begin to contract against the posts. For the majority of the microthrombi observed, the onset of measurable contraction forces was immediate but one clot did exhibit a lag between activation and adhesion, shown as the cyan blue trace in Fig. 6B. It was generally observed that once a clot

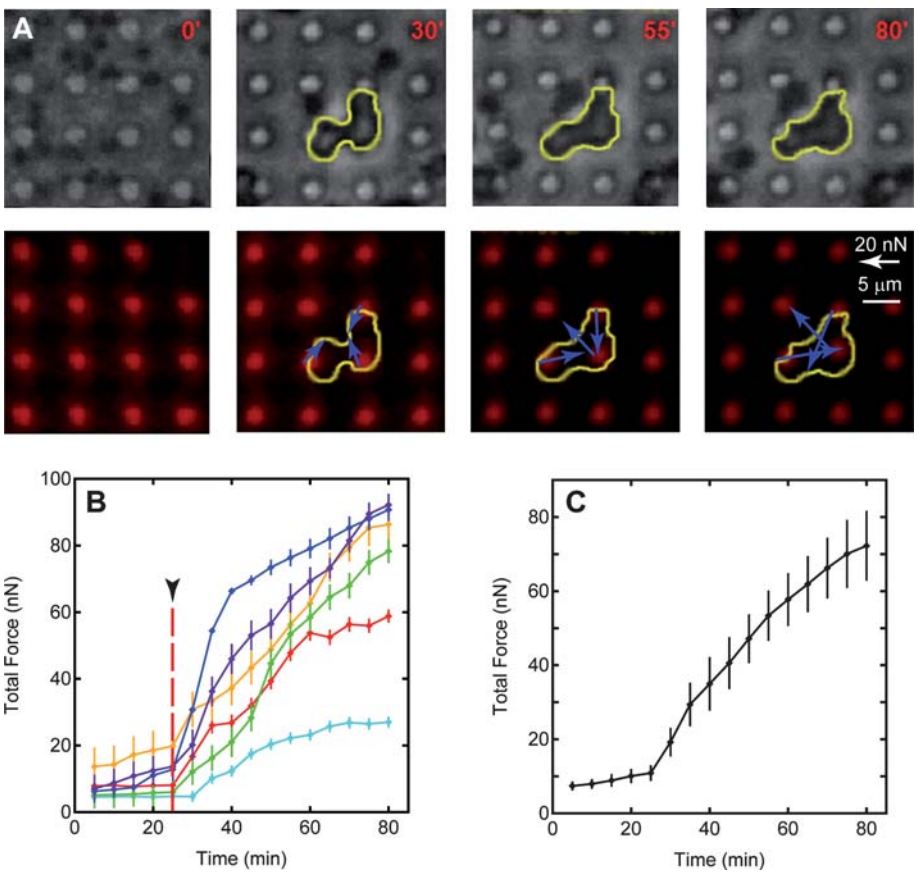

Fig. 6 Live microscopy of thrombus retraction forces. (A) Top row: phase-contrast images of thrombus formation obtained at selected time points. Outline of the clot is shown by yellow trace. Bottom row: fluorescent images of post deflections were used to measure contractile force vectors simultaneously with monitoring of thrombus formation. The clot is not visible under fluorescence, but its outline is shown to illustrate the structural changes in clot formation that accompany the dynamics of contraction force generation. (B) Total force development with time for six clots. Upon thrombin activation at the 25 min mark (arrowhead), all clots exhibit a measureable contractile response. (C) Averaging the total force for all clots in panel B reveals a contractile rate that is similar to the quasi-static measurements shown previously.

was attached, more platelets accumulated onto the thrombus structure with time. Increased aggregation of activated platelets led to an increase in PCF generation, but it was not observed to increase the projected area of each clot in the bright field image. The apparent lack of change in clot size is likely due to incremental growth in the bulk of the thrombus, which would be more readily observed through Z-sectioning than projected area measurements. Unfortunately, it was not feasible to make Z-sectioning measurements during the live imaging of the clotting process because of their longer acquisition time required.

Overall, the phenomena observed confirm that more clotting time enables more platelet aggregation and improved contractile strength. Saturation in PCF was not observed in the average total force for the clots recorded, but a similar monotonic trend in force with time as with the quasi-static PCF measurements was observed (Fig. 6C). Even though contractile development observed in the two approaches is similar, the magnitudes of forces generated were lower in the live microscopy measurements. This may be due to a smaller number of clots recorded as compared to the higher yield in the quasi-static approach. However, it is more likely due to phototoxic inhibition of contractility. For preliminary live microscopy experiments, different video acquisition rates were tried, ranging from one frame captured every 2 s, 30 s, 2 min or 5 min. It was noted that platelets failed to form contractile clots under all frequencies expect for the 5 min acquisition rate. Even though contractile thrombi were observed at this lower illumination time, it is possible that there was reduced contractile force generation due to partial phototoxic effects. However, the similarity between the two approaches corroborates that the flexible post approach is accurate and reliable in measuring PCF. It is also evident that by averaging the forces for a bulk measurement, as seen with the two macroscopic approaches,[21–24] the opportunities in observing individual behavior in platelets, local dynamics, and kinetics of thrombus formation are lost. These phenomena may provide deeper insight in the biophysics of thrombosis and hemostasis.

Discussion

Motivated by the importance of having a strong platelet functional assay, we have developed a new approach to quantitatively measure platelet contractility. Due to the advantages of microfabricated force sensors and confocal microscopy, it was possible for the first time to quantitatively measure platelet contractile forces in individual platelets at the microscale. The ease in biofunctionizing PDMS with matrix proteins on the tips of the posts makes our approach capable of assaying the effects of different matrix ligands on clot adhesion and clot retraction force development. In addition, when combined with live microscopy, visualization of thrombus formation and quantitative micro-clot contraction force development could be correlated to the dynamic events observed during thrombogenesis.

To demonstrate the usefulness of the approach, we performed an extensive series of experiments on soluble and insoluble factors for hemostasis and thrombosis. We observed a critical thrombin concentration in platelet force generation that indicates that physiologically elevated levels of thrombin do not lead to increased contractile response. By treating platelets on the post arrays with other soluble factors, it would be readily straightforward to screen their role on platelet contractile forces. It was also shown that both fibrinogen and fibronectin are able to support similar levels of clotting forces without detachment. This indicates that $\alpha_{IIb}\beta_3$ integrins, which is the common receptor type to both ligands, connects to actin filaments and transmits myosin-derived intracellular forces that lead to retraction forces at the adhesion sites on the posts. It remains to be seen whether other matrix ligands that bind to $\alpha_{IIb}\beta_3$ or other receptors like GP Ib, GP VI, or $\alpha_2\beta_1$ are capable of supporting similar levels of load.

Platelet contractility has been successfully decoupled from fibrin formation and plasma clotting factors, resulting in a contractile measurement that culminates several aspects of platelet function. Measuring PFC requires the successful passage of functional phases like adhesion, activation, shape change, and aggregation that ultimately leads to clot retraction. Specific platelet dysfunction in one of the phases makes it unlikely to generate platelet forces and so measuring PCF can be a critical biophysical metric of overall platelet functionality. The combination of microscale force sensors and isolation of platelets from soluble fibrinogen revealed that individual platelet forces are much larger than previously reported, suggesting that actin–myosin interactions that act on platelet adhesions may have a more significant role in the biomechanics and stability of thrombi than previously regarded. It would be conceivable that internal forces that act at adhesion sites help to recruit additional scaffold proteins[10,11,36] and cluster integrins receptors together to reinforce the strength of the adhesion.[37] There is growing evidence with knockout studies in platelets that mechanotransduction-related focal adhesion proteins like FAK,[38] talin,[39] and kindlin[40] play a critical role in the hemostatic response. Given that externally applied forces to integrins are sufficient to activate focal adhesion protein binding and reinforcement,[41–45] it is foreseeable that internally generated contractile forces could be a similar mechanical factor that regulates thrombus adhesion stability.

In conclusion, the presented platelet microsensor approach has enabled precision measurements of platelet contractile forces under maximal platelet activation. By using different microscopy techniques, either quasi-static platelet contractile force measurements or live imaging, it is possible to study the role of different hemostatic agents or pro-thrombotic factors as they are related to microscale clot behaviors and dynamics of contractile force development. The flexible post force sensor approach for platelets has great potential not only in evaluating platelet hemostatic functionality, but also in studying platelet physiology, anti-platelet drugs, or antithrombotic treatments.

Acknowledgements

We thank Adam Mundy, Wendy Thomas, Paul Wallace, Yueheng Sun, Wes Tooley, and Sunyoung Ahn for helpful discussions and assistance. This work was supported in part by start-up funds from the University of Washington and a National Institutes of Health grant (HL097284). N.J.S. acknowledges the National Science Foundation CAREER award for financial support.

References

1 J. N. George, Platelets, *The Lancet*, 2000, **355**, 1531–1539.
2 P. S. Frenette, R. C. Johnson, R. O. Hynes and D. D. Wagner, Platelets roll on stimulated endothelium *in vivo*: an interaction mediated by endothelial P-selectin, *Proc. Natl. Acad. Sci. U. S. A.*, 1995, **92**, 7450–7454.
3 L. F. Brass, Thrombin and platelet activation, *Chest*, 2003, **124**, 18S–25S.
4 D. L. Bhatt and E. J. Topol, Scientific and therapeutic advances in antiplatelet therapy, *Nat. Rev. Drug Discovery*, 2003, **2**, 15–28.
5 L. F. Brass, L. Zhu and T. J. Stalker, Minding the gaps to promote thrombus growth and stability, *J. Clin. Invest.*, 2005, **115**, 3385–3392.
6 S. P. Jackson, The growing complexity of platelet aggregation, *Blood*, 2007, **109**, 5087–5095.
7 J. W. Weisel, Structure of fibrin: impact on clot stability, *J. Thromb. Haemost.*, 2007, **1**(5), 116–124.
8 B. Geiger, A. Bershadsky, R. Pankov and K. M. Yamada, Transmembrane extracellular matrix–cytoskeleton crosstalk, *Nat. Rev. Mol. Cell Biol.*, 2001, **2**, 793–805.
9 I. Cohen, The contractile system of blood platelets and its function, *Methods Achiev. Exp. Pathol.*, 1979, **9**, 40–86.
10 V. T. Nachmias and R. Golla, Vinculin in relation to stress fibers in spread platelets, *Cell Motil. Cytoskeleton*, 1991, **20**, 190–202.
11 J. Hagmann, Pattern formation and handedness in the cytoskeleton of human platelets, *Proc. Natl. Acad. Sci. U. S. A.*, 1993, **90**, 3280–3283.
12 J. Hagmann, M. Grob, A. Welman, G. van Willigen and M. M. Burger, Recruitment of the LIM protein hic-5 to focal contacts of human platelets, *J. Cell Sci.*, 1998, **111**(Pt 15), 2181–2188.
13 S. D. J. Calamiunus, J. M. Auger, O. J. T. McCarty, M. J. O. Wakelam, L. M. Machesky and S. P. Watson, MyosinIIa contractility is required for maintenance of platelet structure during spreading on collagen and contributes to thrombus stability, *J. Thromb. Haemost.*, 2007, **5**, 2136–2145.
14 A. Ono, E. Westein, S. Hsiao, W. S. Nesbitt, J. R. Hamilton, S. M. Schoenwaelder and S. P. Jackson, Identification of a fibrin-independent platelet contractile mechanism regulating primary hemostasis and thrombus growth, *Blood*, 2008, **112**, 90–99.
15 C. Leon *et al.*, Megakaryocyte-restricted MYH9 inactivation dramatically affects hemostasis while preserving platelet aggregation and secretion, *Blood*, 2007, **110**, 3183–3191.
16 M. E. Carr, Jr, Development of platelet contractile force as a research and clinical measure of platelet function, *Cell Biochem. Biophys.*, 2003, **38**, 55–78.
17 P. Harrison, Platelet function analysis, *Blood Rev.*, 2005, **19**, 111–123.
18 R. Cardigan, C. Turner and P. Harrison, Current methods of assessing platelet function: relevance to transfusion medicine, *Vox Sang.*, 2005, **88**, 153–163.
19 N. Katori, K. A. Tanaka, F. Szlam and J. H. Levy, The effects of platelet count on clot retraction and tissue plasminogen activator-induced fibrinolysis on thrombelastography, *Anesth. Analg.*, 2005, **100**, 1781–1785.
20 M. T. Ganter and C. K. Hofer, Coagulation monitoring: current techniques and clinical use of viscoelastic point-of-care coagulation devices, *Anesth. Analg.*, 2008, **106**, 1366–1375.
21 I. Cohen and A. De Vries, Platelet contractile regulation in an isometric system, *Nature*, 1973, **246**, 36–37.
22 C. J. Jen and L. V. McIntire, The structural properties and contractile force of a clot, *Cell Motil.*, 1982, **2**, 445–455.
23 L. Salganicoff, M. H. Loughnane, R. W. Sevy and M. Russo, The platelet strip. I. A low-fibrin contractile model of thrombin-activated platelets, *Am. J. Physiol.*, 1985, **249**, C279–287.
24 M. E. Carr, Jr and S. L. Zekert, Measurement of platelet-mediated force development during plasma clot formation, *Am. J. Med. Sci.*, 1991, **302**, 13–18.
25 P. E. Greilich, M. E. Carr, Jr, S. L. Carr and A. S. Chang, Reductions in platelet force development by cardiopulmonary bypass are associated with hemorrhage, *Anesth. Analg.*, 1995, **80**, 459–465.
26 M. E. Carr, Jr, M. H. Hackney, S. J. Hines, S. P. Heddinger, S. L. Carr and E. J. Martin, Enhanced platelet force development despite drug-induced inhibition of platelet aggregation in patients with thromboangiitis obliterans—two case reports, *Vasc. Endovasc. Surg.*, 2002, **36**, 473–480.
27 I. Cohen, J. M. Gerrard and J. G. White, Ultrastructure of clots during isometric contraction, *J. Cell Biol.*, 1982, **93**, 775–787.
28 M. E. Carr, Jr, R. M. Dent and S. L. Carr, Abnormal fibrin structure and inhibition of fibrinolysis in patients with multiple myeloma, *J. Lab. Clin. Med.*, 1996, **128**, 83–88.
29 J. L. Tan, J. Tien, D. M. Pirone, D. S. Gray, K. Bhadriraju and C. S. Chen, Cells lying on a bed of microneedles: an approach to isolate mechanical force, *Proc. Natl. Acad. Sci. U. S. A.*, 2003, **100**, 1484–1489.
30 O. du Roure, A. Saez, A. Buguin, R. H. Austin, P. Chavrier, P. Siberzan and B. Ladoux, Force mapping in epithelial cell migration, *Proc. Natl. Acad. Sci. U. S. A.*, 2005, **102**, 2390–2395.
31 N. J. Sniadecki and C. S. Chen, Microfabricated silicone elastomeric post arrays for measuring traction forces of adherent cells, *Meth. Cell Biol.*, 2007, **83**, 313–328.
32 C. A. Lemmon, N. J. Sniadecki, S. A. Ruiz, J. L. Tan, L. H. Romer and C. S. Chen, Shear force at the cell-matrix interface: enhanced analysis for microfabricated post array detectors, *Mech. Chem. Biosyst.*, 2005, **2**, 1–16.
33 N. J. Sniadecki, C. M. Lamb, Y. Liu, C. S. Chen and D. H. Reich, Magnetic microposts for mechanical stimulation of biological cells: fabrication, characterization, and analysis, *Rev. Sci. Instrum.*, 2008, **79**, 044302.
34 G. E. Jarvis, B. T. Atkinson, J. Frampton and S. P. Watson, Thrombin-induced conversion of fibrinogen to fibrin results in rapid platelet trapping which is not dependent on platelet activation or GPIb, *Br. J. Pharmacol.*, 2003, **138**, 574–583.
35 B. Savage, S. J. Shattil and Z. M. Ruggeri, Modulation of platelet function through adhesion receptors. A dual role for glycoprotein IIb–IIIa (integrin alpha IIb beta 3) mediated by fibrinogen and glycoprotein Ib-von Willebrand factor, *J. Biol. Chem.*, 1992, **267**, 11300–11306.
36 J. Hagmann, M. Grob, A. Welman, G. van Willigen and M. M. Burger, Recruitment of the LIM protein hic-5 to focal contacts of human platelets, *J. Cell Sci.*, 1998, **111**(Pt 15), 2181–2188.
37 S. J. Shattil, H. Kashiwagi and N. Pampori, Integrin signaling: the platelet paradigm, *Blood*, 1998, **91**, 2645–2657.
38 I. S. Hitchcock, N. E. Fox, N. Prevost, K. Sear, S. J. Shattil and K. Kaushansky, Roles of focal adhesion kinase (FAK) in megakaryopoiesis and platelet function: studies using a megakaryocyte lineage specific FAK knockout, *Blood*, 2008, **111**, 596–604.
39 B. G. Petrich, P. Marchese, Z. M. Ruggeri, S. Spiess, R. A. M. Weichert, F. Ye, R. Tiedt, R. C. Skoda, S. J. Monkley, D. R. Critchley and M. H. Ginsberg, Talin is required for integrin-mediated platelet function in hemostasis and thrombosis, *J. Exp. Med.*, 2007, **204**, 3103–3111.
40 M. Moser, B. Nieswandt, S. Ussar, M. Pozgajova and R. Fassler, Kindlin-3 is essential for integrin activation and platelet aggregation, *Nat. Med.*, 2008, **14**, 325–330.
41 D. Riveline, E. Zamir, N. Q. Balaban, U. S. Schwarz, T. Ishizaki, S. Narumiya, Z. Kam, B. Geiger and A. D. Bershadsky, Focal contacts as mechanosensors: externally applied local mechanical force induces growth of focal contacts by an mDia1-dependent and ROCK-independent mechanism, *J. Cell Biol.*, 2001, **153**, 1175–1186.
42 C. G. Galbraith, K. M. Yamada and M. P. Sheetz, The relationship between force and focal complex development, *J. Cell Biol.*, 2002, **159**, 695–705.
43 Y. Sawada and M. P. Sheetz, Force transduction by Triton cytoskeletons, *J. Cell Biol.*, 2002, **156**, 609–615.
44 N. J. Sniadecki, A. Anguelouch, M. T. Yang, C. M. Lamb, Z. Liu, S. B. Kirschner, Y. H. Liu, D. H. Reich and C. S. Chen, Magnetic microposts as an approach to apply forces to living cells, *Proc. Natl. Acad. Sci. U. S. A.*, 2007, **104**, 14553–14558.
45 A. del Rio, R. Perez-Jimenez, R. Liu, P. Roca-Cusachs, J. M. Fernandez and M. P. Sheetz, Stretching single talin rod molecules activates vinculin binding, *Science*, 2009, **323**, 638–641.